Received: 16 July 2020 | Revised: 22 January 2021 | Accepted: 31 January 2021

DOI: 10.1111/ejn.15138

SPECIAL ISSUE ARTICLE

EJN European Journal of Neuroscience FENS WILEY

Pre-stimulus alpha-band power and phase fluctuations originate from different neural sources and exert distinct impact on stimulus-evoked responses

Agnese Zazio[1] | **Philipp Ruhnau**[2,3] | **Nathan Weisz**[3,4] | **Andreas Wutz**[4]

[1]Neurophysiology Lab, IRCCS Istituto Centro San Giovanni di Dio Fatebenefratelli, Brescia, Italy

[2]Department of Neurology, Otto-von-Guericke University Magdeburg, Magdeburg, Germany

[3]Center for Mind/Brain Sciences – CIMeC, University of Trento, Rovereto, Italy

[4]Centre for Cognitive Neuroscience, University of Salzburg, Salzburg, Austria

Correspondence
Agnese Zazio, Neurophysiology Lab, IRCCS Istituto Centro San Giovanni di Dio Fatebenefratelli, Via Pilastroni 4, 25125 Brescia, Italy.
Email: agnese.zazio@cognitiveneuroscience.it

Funding information
Austrian Science Fund, Grant/Award Number: M2496; H2020 European Research Council, Grant/Award Number: ERC StG 283404 – WIN2CON; Ministero della Salute

Abstract

Ongoing oscillatory neural activity before stimulus onset influences subsequent visual perception. Specifically, both the power and the phase of oscillations in the alpha-frequency band (9–13 Hz) have been reported to predict the detection of visual stimuli. Up to now, the functional mechanisms underlying pre-stimulus power and phase effects on upcoming visual percepts are debated. Here, we used magnetoencephalography recordings together with a near-threshold visual detection task to investigate the neural generators of pre-stimulus power and phase and their impact on subsequent visual-evoked responses. Pre-stimulus alpha-band power and phase opposition effects were found consistent with previous reports. Source localization suggested clearly distinct neural generators for these pre-stimulus effects: Power effects were mainly found in occipital-temporal regions, whereas phase effects also involved prefrontal areas. In order to be functionally relevant, the pre-stimulus correlates should influence post-stimulus processing. Using a trial-sorting approach, we observed that only pre-stimulus power modulated the Hits versus Misses difference in the evoked response, a well-established post-stimulus neural correlate of near-threshold perception, such that trials with stronger pre-stimulus power effect showed greater post-stimulus difference. By contrast, no influence of pre-stimulus phase effects were found. In sum, our study shows distinct generators for two pre-stimulus neural patterns predicting visual perception, and that only alpha power impacts the post-stimulus correlate of conscious access. This underlines the functional relevance of prestimulus alpha power on perceptual awareness, while questioning the role of alpha phase.

KEYWORDS

conscious perception, magnetoencephalography, neural oscillations, phase opposition, visual detection

Abbreviations: BA, Brodmann area; EEG, electroencephalography; ERFs, event-related fields; ITC, inter-trial coherence; LCMV, Linearly Constrained Minimum Variance; MEG, magnetoencephalography; MNI, Montreal Neurological Institute; POS, phase opposition sum.

Edited by: Niko Busch

1 | INTRODUCTION

Spontaneous fluctuations in neural oscillatory activity that precede the presentation of a sensory stimulus impact conscious perception in the visual (Benwell, et al., 2018; Benwell, Tagliabue, et al., 2017; Chaumon & Busch, 2014; Dugué et al., 2011; Hanslmayr et al., 2007; Rassi et al., 2019; Romei et al., 2008; Samaha et al., 2017; van Dijk et al., 2008; Wutz et al., 2014), auditory (Frey et al., 2014; Henry & Obleser, 2012), and somatosensory domain (Ai & Ro, 2014; Baumgarten et al., 2016; Linkenkaer-Hansen et al., 2004; Weisz et al., 2014). Typically, neuroscience research investigating the effects of pre-stimulus oscillations employ "near-threshold" stimuli, whose intensity is set at an individual sensory threshold, with the aim of maximizing response variability in conscious report while avoiding confounding factors related to the physical properties of the stimuli. By definition, repeatedly presented near-threshold stimuli are detected in approximately half of the trials. Generally, trials in which the target-stimuli were successfully detected (i.e., Hits) are associated with a greater evoked response compared to trials in which the target-stimuli were missed (i.e., Misses). These post-stimulus differences are a hallmark of conscious perception of near-threshold stimuli (Dehaene & Changeux, 2011; Sanchez et al., 2020).

Especially in the visual domain, pre-stimulus oscillations in the alpha-frequency band (9–13 Hz), as measured by means of electro- and -magneto-encephalographic recordings (EEG and MEG; for a review see Ruhnau et al., 2014), play a key role. Numerous studies have demonstrated that pre-stimulus alpha-band power inhibits perceptual awareness, with a reduced probability of detecting a near-threshold stimulus on trials with high alpha-band power in the pre-stimulus window (Ergenoglu et al., 2004; Iemi et al., 2017; Limbach & Corballis, 2016; Samaha et al., 2017; van Dijk et al., 2008; Wutz et al., 2014; Wyart & Tallon-Baudry, 2008). Furthermore, it has been shown that perceptual outcome is also influenced by the phase of alpha-band oscillations in the pre-stimulus window (Busch et al., 2009; Busch & Van Rullen, 2010; Mathewson et al., 2009), supporting the idea of discrete sampling of visual processing (VanRullen, 2016a). Taken together, findings on pre-stimulus power and phase have led to the development of multiple frameworks relying on the core concept of pulsed-inhibition exerted by oscillatory brain activity in the alpha band (Jensen et al., 2014; Jensen & Mazaheri, 2010; Klimesch et al., 2007; Mathewson et al., 2011; Schalk, 2015; Zazio et al., 2020). Nevertheless, so far it is still unclear whether pre-stimulus alpha-band power and phase reflect the same or different mechanisms. In particular, little is known about the neural sources of pre-stimulus oscillations and how they impact the post-stimulus response.

The modelling of brain sources involved in pre-stimulus oscillatory effects is of particular importance, given recent findings showing that neural activity in several stages along the visual stream is crucial for conscious report, from early sensory areas to higher-order frontal regions (Andersen et al., 2016; Van Vugt et al., 2018). Previous work on pre-stimulus alpha-band activity suggests the involvement of both posterior brain regions as well as parietal and frontal areas (Busch et al., 2009; Dugué et al., 2011; Hanslmayr et al., 2007, 2011; Iemi et al., 2017; Limbach & Corballis, 2016; Mathewson et al., 2009; Romei et al., 2008; Samaha et al., 2017; Thut et al., 2006; van Dijk et al., 2008). However, many findings reported so far arise from EEG recordings (for MEG evidence see: Rassi et al., 2019; van Dijk et al., 2008; Wutz et al., 2018) and/or focus on a single feature of ongoing alpha activity (i.e., power or phase), resulting in an incomplete picture of the brain areas involved in ongoing alpha-band oscillations and leaving the question open whether the effects of power and phase originate from the same brain areas. Furthermore, only very few studies specifically investigated interactions between pre-stimulus alpha-band oscillations and stimulus-evoked response (for example see Wutz et al., 2014): if pre-stimulus alpha activity is functionally relevant for conscious perception, then we would expect it to impact not only the perceptual outcome (i.e., Hit and Miss response), but also the classic neural correlates of conscious access (i.e., the stimulus-evoked neural activity).

In this study, we first aimed at replicating the impact of spontaneous fluctuations in pre-stimulus alpha-band power and phase on visual perception found previously, by adopting a near-threshold visual detection paradigm similar to the one reported in Busch et al. (2009). Importantly, however, the MEG recordings together with brain source modelling used here enabled us to advance on previous EEG evidence by examining these effects at the brain source level. Second, we compared Hits and Misses in pre-stimulus alpha-band power, pre-stimulus alpha-band phase and in the stimulus-evoked response (i.e., event-related fields, ERFs) with particular emphasis on how pre-stimulus features shape post-stimulus neural correlates of conscious detection. This strategy allowed us to more thoroughly map out the neural basis of pre-stimulus power and phase effects and their functional impact on visual percepts and visual-evoked responses.

2 | MATERIALS AND METHODS

2.1 | Participants

Twenty healthy volunteers took part in the study after giving written informed consent (12 female, mean age ± *SD*:

26 ± 4 years, all right-handed). All participants had normal or corrected-to-normal vision and no history of neurological disorders. The study was conducted in accordance with the Declaration of Helsinki and approved by the local ethics committee of the University of Trento.

2.2 | Apparatus

2.2.1 | Stimulus presentation

Stimuli were generated using MATLAB 2012b (The MathWorks) and Psychophysics Toolbox 3 (Brainard, 1997; Pelli, 1997). A DLP projector (PROPixx; VPixx Technologies) showed the stimuli at a refresh rate of 120 Hz centred onto a translucent screen. The screen was located in front of the participant (viewing distance, 150 cm) within the dimly lit, magnetically shielded MEG room. Stimulus timing was controlled with a data and video processing peripheral (DATAPixx; VPixx Technologies) and monitored via a photo diode placed at the upper left corner of the projection screen. The delay between trigger and stimulation onset was corrected using the photodiode information.

2.2.2 | MEG recordings

Whole-head MEG was continuously recorded with a sampling rate of 1 kHz (Neuromag306 system; Elekta), placed in a magnetically shielded room. MEG data was recorded by 306 sensors (one magnetometer and two orthogonal planar gradiometers for each of 102 positions). For each participants, a Polhemus Fastrack digitizer was used to acquire the location of a set of landmarks: nasion and left/right periauricular points, five head position indicator (HPI) coils to track the position of the participants' head during the experiment, and more than 200 head shape samples, needed for offline head shape modelling.

2.3 | Stimuli and experimental procedure

Participants were comfortably seated in a dimly lit, sound attenuated and magnetically shielded room. The visual detection task was similar to the one described in Busch et al., (2009; Figure 1a). A fixation cross was always present in the center of the screen, while two lateral markers on its right side (7° of visual angle eccentricity) indicated the

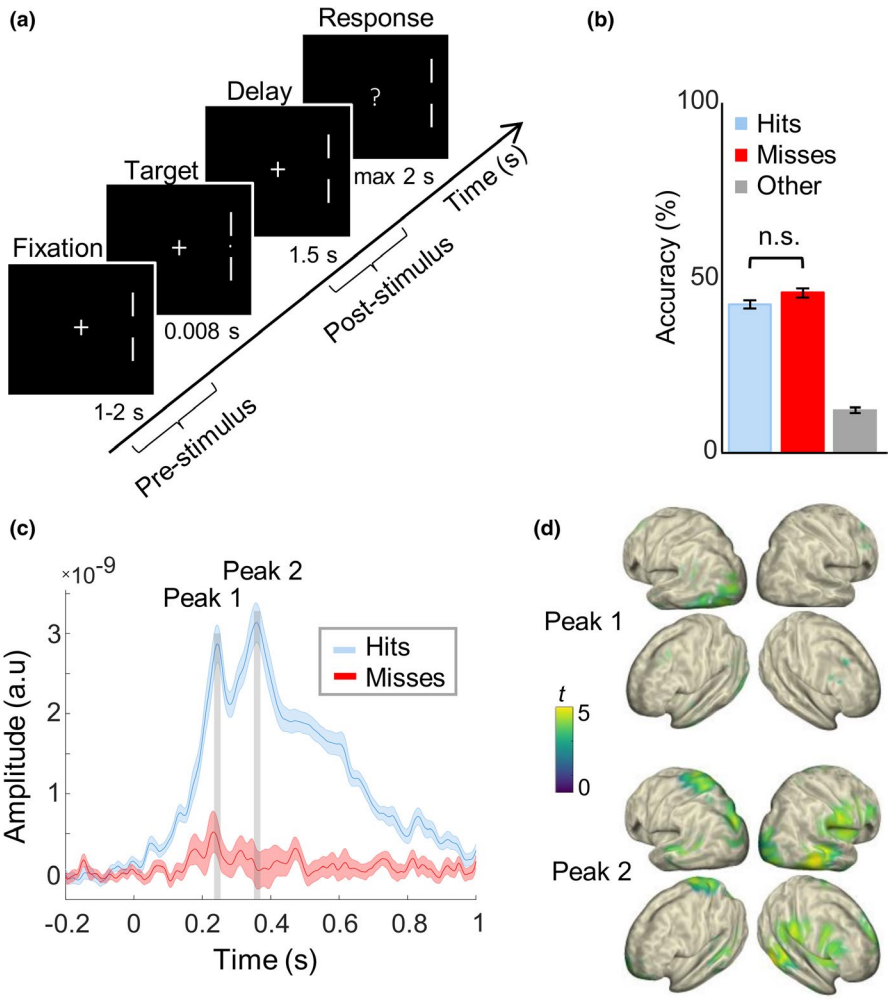

FIGURE 1 Visual detection task and evoked response. (a) Trial structure: while keeping eye fixation on the cross located in the center of the screen, participants were asked to detect a small dot that could appear in 80% of the trials between two markers, located on the right side of the screen. (b) Detection performance at chance level for Hits and Misses; other responses included False alarms and no-response trials (e.g., within-subject *SE* in error bars; Morey, 2008). (c) Time course of ERFs (baseline corrected for visualization purpose) showing a significantly larger response for Hits than Misses, averaged over significant virtual sensors in the cluster at the two peaks; within-subjects *SE* in shaded error bars (Morey, 2008). (d) Source plots of significant *t* values in the cluster at the two ERF peaks. For visualization purposes, data has been interpolated over virtual sensors and the threshold for significance was set at $t = 4.2$, $p < .001$

location in which the target could appear. Participants were asked to maintain fixation, while covertly attending the lateral site indicated by the markers. The target was presented in 80% of the trials, after a variable interval between 1 and 2 s after fixation onset, so that target onset was unpredictable. The target was a small dot (7′ of visual angle), which was briefly presented (for 8.3 ms, i.e., one frame) at individual luminance threshold (i.e., 50% of detection accuracy; determined before the MEG recording with a staircase procedure for each participant). A question mark appeared 1.5 s after the target presentation and the participants were asked to report whether they detected the target or not by pressing the left and the right key on an MEG compatible button pad (RESPONSEPixx; VPixx Technologies), with the index and middle finger of their dominant hand, respectively. The buttons were counterbalanced across subjects. A new trial began after the response, or after 2 s if no response was recorded. Participants performed 6 blocks of 150 trials each (due to technical reasons, two participants only completed 4 blocks); a brief pause of a few minutes was provided between blocks to avoid drops of attention and alertness throughout the experiment. The experiment lasted approximately 1.5 hr.

2.4 | Data analysis

2.4.1 | Behavioral data

Detection performance was evaluated in terms of Hits (i.e., number correct detections on the total of presented targets) and Misses (i.e., rate of missed targets). The false alarm rate was estimated based on target-absent trials (20% trials).

2.4.2 | MEG data

Preprocessing

Magnetoencephalography data analysis was performed in MATLAB 2016b (The MathWorks), using the FieldTrip toolbox (Oostenveld et al., 2011) and the CircStat toolbox (Berens, 2009). The MEG signal was high pass filtered at 1 Hz and a notch filter at 50 Hz and 100 Hz was applied to remove line noise. Data were downsampled to 256 Hz and epoched from 2 s before to 2 s after stimulus onset. A set of summary statistics (variance, maximum absolute amplitude, maximum z value) was used to detect and then remove outliers of channels and trials. Moreover epochs were visually inspected and noisy channels as well as trials with residual artifacts (noise, eye movements and muscular artifacts), were removed (semi-automatic artifact rejection). On average, $10 \pm 2\%$ of the trials and 4 ± 2 channels were discarded (mean $\pm$ *SD*). For every subject, the number of trials for Hits and Misses was equalized by randomly selecting a subset of trials from the condition with more trials, because phase calculation is sensitive to trial number (VanRullen, 2016b). Target-absent trials as well as trials with no response were excluded.

Source-projection

Pre-processed sensor data was projected into source space. For each participant, we performed the co-registration between anatomical and MEG channels using the individual MRI and the landmarks recorded prior to acquisition. Only MEG gradiometer data was used. A structural magnetic resonance image (MRI) was available for 15 of 20 participants. For the remaining subjects, we obtained the canonical cortical anatomy from the affine transformation of a Montreal Neurological Institute (MNI)-template brain (Montreal, Canada; brainweb.bic.mni.mcgill.ca/brainweb/) to the subject's digitized head shape. A single shell head model (Nolte, 2003) was used to represent the geometrical and electro-magnetic properties of the head. Then, we constructed the source model by using a spatial grid of 889 points with a resolution of 15 mm in MNI space, which was warped into the individual head model. In this way, the data from each subject was mapped onto a common space. Finally, a Linearly Constrained Minimum Variance (LCMV) beamformer filter (Van Veen et al., 1997) was applied to the single-trial data, using a covariance window from −0.3 s to −0.1 s with respect to stimulus onset. Anatomical structures corresponding to localized sources were identified using the MNI brain and Talairach atlas (MRC Cognition and Brain Sciences Unite, Cambridge, UK; imaging.mrc-cbu.cam.ac.uk/imaging/MniTalairach).

Event-related fields

Event-related fields were computed by low pass filtering the signal at 20 Hz and averaging over trials for Hits and Misses. Polarity was discarded by taking the absolute value of ERFs.

Time-frequency representations

Time–frequency representations (fast Fourier transform) were calculated on single-trial data using Hanning tapers applied to short sliding time windows in steps of 10 ms in the frequency range between 1 and 30 Hz. We used a frequency-dependent window width of five cycles per frequency. The squared absolute value of the Fourier estimates gave the signal power. Phase coherence across trials was quantified with the inter-trial coherence metric (ITC; Lachaux et al., 1999). To control for difference in amplitude across trials and extract only the information about phase, the length of the complex vectors resulting from Hanning tapering and Fourier transform was normalized to 1 across all trials. Then, ITC was calculated as the length of the resultant complex Fourier vectors across trials along the unit circle. The range of ITC values is between 0 and 1, with 0 representing random phase angle distributions and 1 perfect phase-locking across

trials. Phase coherence with ITC was calculated separately for trial subsets for Hits (ITC_{HITS}), Misses (ITC_{MISSES}) and comprising Hits and Misses together (ITC_{ALL}). To quantify phase opposition between the trial subsets, we used the Phase Opposition Sum (POS, defined in (1)), which has been shown to be more reliable compared to other measures (e.g., Phase Bifurcation Index; VanRullen, 2016b).

$$POS = ITC_{HITS} + ITC_{MISSES} - 2 \times ITC_{ALL} \quad (1)$$

POS values are positive only when both Hits and Misses are phase locked and have opposite phase angles. We used a permutation approach to test whether the POS values were significantly greater than expected by chance (see *Permutation statistics for POS*). In all other cases (i.e., only one condition presents high ITC, both conditions present low ITC, or both conditions present high ITC but with similar phase angles), POS values are not statistically different from chance.

Effect of pre-stimulus alpha power on the evoked response

To investigate the impact of pre-stimulus alpha power on ERFs, we selected subsets of trials, in which the power effect was "maximized" or "minimized," respectively. To this end, we averaged power over the alpha-frequency band (9–13 Hz) and across the pre-stimulus time points from −0.45 s to −0.3 s (i.e., the time range in which the power effect was found to be maximal). Trial sorting was performed in two ways: (a) based on the data at the virtual sensor that shows the strongest power difference between Hits and Misses, which was located in occipital-temporal cortex (Figure S1a), and (b) based on the data averaged over all significant virtual sensors in the contrast between Hits and Misses. In both analyses, we selected 30% of Hit trials with the lowest pre-stimulus alpha power and 30% of Misses with the highest pre-stimulus alpha power to "maximize" the effect ($POW_{MAX\text{-}EFFECT}$). Conversely, in order to "minimize" the effect, we selected the 30% of Hits with the highest pre-stimulus alpha power and the 30% of Misses with the lowest pre-stimulus alpha power ($POW_{MIN\text{-}EFFECT}$). The trial subsets for both power and phase were balanced with respect to the trial numbers for Hits and Misses for each participant. On average, the new subsets comprised 83 trials (minimum trial number: 55). Then, ERFs were calculated at all virtual sensors and time points from 0.2 s before to 0.8 s after stimulus onset, following the same steps as reported above, for each trial subset. The two analyses lead to similar results.

Effect of pre-stimulus alpha phase on the evoked response

The effect of pre-stimulus alpha POS on ERFs was investigated as follows. Following the same reasoning that we applied to the analysis of pre-stimulus alpha power, our aim was to maximize and minimize the effect of pre-stimulus alpha phase opposition. Therefore, POS was calculated as described above, and trial sorting was performed in different ways. First, trial sorting was performed based on the data at the two virtual sensors that showed the highest POS values in the analysis of pre-stimulus alpha phase, which were located in two spatially distant regions in the left visual and in the right prefrontal cortex (Figure S1b,c). Considering that phase, by definition, is not stationary over time, we calculated the mean phase angles over Hit- and Miss-trials at the middle frequency and time point in the range of interest, that is, at 11 Hz and at 200 ms before stimulus onset. We expected to find the strongest differences at these single spatial-spectral-time points; however, this selection could be too narrowly focused. Therefore, trial sorting was additionally performed by (a) averaging over all significant virtual sensors for the phase effect and (b) by averaging over the whole time-frequency range of the POS statistics, that is, from −0.3 to −0.1 s before stimulus onset and between 9 and 13 Hz. In all the analyses, the effect of pre-stimulus phase opposition was maximized by selecting the 30% of trials with phase angles closest to the mean phase angle within Hits and Misses ($POS_{MAX\text{-}EFFECT}$), respectively, and minimized by selecting the 30% of trials with phase angles close to ±90° from its mean phase angle ($POS_{MIN\text{-}EFFECT}$; a schematic representation that explains the rationale of the POS trial sorting approach in more detail can be found in Figure S2). Then, ERFs for $POS_{MAX\text{-}EFFECT}$ and $POS_{MIN\text{-}EFFECT}$ were calculated at all virtual sensors and time points from 0.2 s before to 0.8 s after stimulus onset, as described above. All the analyses lead to similar results.

2.4.3 | Statistical analysis

Behavioral data analysis

The behavioral analysis of Hit- and Miss-rates was performed by means of dependent samples *t* tests. Moreover, a repeated-measure analysis of variance (rm-ANOVA) with 6-level factor Block was run to test for an alertness decrease throughout the experiment. This analysis included 18 out of 20 participants who completed the 6 experimental blocks.

Non-parametric cluster-based permutation statistics for ERFs and power

Magnetoencephalography data for Hits and Misses in ERFs and pre-stimulus power were compared by performing non-parametric cluster-based permutation tests for dependent samples (two-tailed *t* statistics; Maris & Oostenveld, 2007). This procedure allows controlling for the multiple comparisons problem (type I error), arising when performing statistical tests at multiple time points and sensors. First, it identifies significant spatio-temporal adjacent clusters, summing *t*-values within each cluster to reveal a cluster-level test

statistic. Then, it performs random permutations by exchanging the data between Hits and Misses within participants. After each permutation run, the maximum cluster level statistic was recorded to obtain a reference distribution of cluster-level statistics (approximated with Monte Carlo procedure of 1,000 permutations). Finally, cluster-level *p*-values were estimated as the proportion of values in the reference distribution exceeding the cluster-statistics obtained in the real data. The level of significance was set at $p < .05$.

The non-parametric cluster-based permutation was used to compare the ERFs between Hits and Misses over all virtual sensors and the time points from −0.2 s before to 0.8 s after stimulus onset. The same analysis (Hits vs. Misses) was applied separately to the trial subsets arising from trial sorting for maximization/minimization of pre-stimulus alpha power (i.e., $POW_{MAX\text{-}EFFECT}$ and $POW_{MIN\text{-}EFFECT}$) and phase (i.e., $POS_{MAX\text{-}EFFECT}$ and $POS_{MIN\text{-}EFFECT}$) and for the difference between Hits and Misses for each trial subset. The difference in alpha-band power (averaged between 9–13 Hz) between Hits and Misses was tested with the non-parametric cluster-based permutation procedure over the pre-stimulus time window (−0.5 to 0 s before stimulus onset) and across all virtual sensors. The cluster-based permutations over virtual sensors and time-points were performed also to compare Hits and Misses in the ERFs baseline (−0.5 to 0 s before stimulus onset), and in the post-stimulus alpha power (averaged between 9–13 Hz; see Supplementary Materials). Finally, the Hits-Misses difference was calculated to test the relationship between ERF amplitude and post-stimulus alpha power at the latency of the two ERF peaks, by means of Pearson correlation (see Supplementary Materials).

Permutation statistics for POS

The statistical analysis of POS between Hits and Misses followed the approach reported by Busch et al. (2009). First, we re-calculated POS for "pseudo-Hits" and "pseudo-Misses" trial subsets drawn randomly from a merged pool of all trials for each participant. This procedure was repeated 500 times, giving rise to a shuffled POS distribution under the null hypothesis for each participant. The same trials were considered in the computation of the real and the shuffled data. In a second step, we randomly selected one permutation out of the 500 POS per participant, and computed the grand-average across participants. The second step was performed 10,000 times. Finally, we computed *p*-values as the proportion of shuffled POS grand-averages that exceeded the observed POS grand-average. The level of significance was set at $p < .05$. Phase opposition was tested across all virtual sensors for the average POS over the alpha frequency band (9–13 Hz) immediately before stimulus onset (−0.3 s to −0.1 s, consistent with the locus of the effects found in Busch et al., 2009). The false discovery rate (FDR) procedure (Benjamini & Hochberg, 1995) was applied, in order to correct for multiple comparisons over virtual sensors. Finally, the same statistical steps were performed on new subsets of Hits and Misses which have been stratified for pre-stimulus alpha power, to rule out possible confounds of power in the estimation of POS (see Supplementary Materials).

Repeated-measures ANOVAs for max-effect and min-effect subgroups

The ERF peak amplitudes were averaged across all significant virtual sensors and ±20 ms around each peak identified from the ERF grand-average for both Hits and Misses in $POW_{MAX\text{-}EFFECT}$ and $POW_{MIN\text{-}EFFECT}$. The effects of pre-stimulus alpha power on the evoked response at the two ERF peaks was investigated by means of 2 × 2 rm-ANOVAs with the factors Response (Hits, Misses) and Effect ($POW_{MAX\text{-}EFFECT}$, $POW_{MIN\text{-}EFFECT}$). The same statistical model was applied to POS data (factors: Response—Hits, Misses—and Effect—$POS_{MAX\text{-}EFFECT}$ and $POS_{MIN\text{-}EFFECT}$) calculated at the two virtual sensors of interest (i.e., in left visual and right prefrontal cortex).

3 | RESULTS

As expected, participants detected on average around half of the near-threshold visual targets, with no difference between Hits and Misses (mean ± *SE* for repeated measures (Morey, 2008): Hit rate: 42.3 ± 1.1%; Miss rate: 45.6 ± 1.2%; $t = 1.49$, $p = .154$; Figure 1b). Because in a few trials we recorded no response (which may have been provided too early, i.e., before the question mark appearance, too late, i.e., after 2 s with respect to the time interval for the response, or may have not been provided at all), the sum of the Hit- and Miss rates was not 100%. Performance did not vary significantly between the experimental blocks ($F_{5,85} = 1.55$, $p = .18$), suggesting that alertness did not decrease throughout the experiment. Moreover, the false alarm rate was very low (2.5% ± 0.6), indicating that participants' response reflected actual detection. The stimulus-evoked response on Hit-trials was significantly larger than on Miss-trials (cluster-corrected $p = .002$; Figure 1c). The time course of ERFs on Hit-trials showed two clear peaks: an earlier one at ~0.24 s, mostly involving left occipital areas contralateral to the target location (maximum *t* value located in left occipital cortex, Brodmann area (BA) 19; $t_{MAX} = 4.69$; MNI coordinates in mm: −20, –65, –5). Then, there was a later peak at ~0.36 s, showing more wide-spread activity across parietal and temporal areas and also extending to the right hemisphere (maximum *t*-value located in right supramarginal gyrus, in parietal cortex BA 40; $t_{MAX} = 4.84$; MNI coordinates in mm: 70, –20, 25; Figure 1d). Hits and Misses did not differ in the pre-stimulus baseline ($p > .42$, see Supplementary Materials and Figure S3a). Furthermore, the

analysis of power in the post-stimulus window showed lower alpha power levels in Hits than Misses (cluster-corrected $p = .002$; see Supplementary Materials and Figure S3b), and no significant correlation was observed between ERF amplitude and post-stimulus alpha power at the latency of the two ERF peaks (all abs (r) < .14, all $p > .58$, see Supplementary Materials and Figure S3c).

Next, we investigated alpha-band fluctuations and their influence on the perceptual outcome on the brain source-level by computing time-frequency analyses in the time window preceding stimulus onset (−0.5 –0 s) for Hit- and Miss-trials. First, in line with previous work (Busch et al., 2009; Limbach & Corballis, 2016) we found that lower alpha power levels preceded Hits compared to Misses peaking at ~0.36 s before target onset (cluster-corrected $p = .01$; Figure 2a). Brain source results (Van Veen et al., 1997) revealed the strongest effects over occipital-temporal areas, which were lateralized to the left hemisphere, contralateral to stimulus presentation (minimum t value in the left occipital cortex, BA 39; $t_{MIN} = -3.64$; MNI coordinates in mm: −50, −65, 10; Figure 2b). Second, confirming previous reports (Busch et al., 2009; Mathewson et al., 2009) we found oscillatory alpha-band activity just before stimulus onset (−0.3 to −0.1 s) to be phase locked with opposed phase angles on Hit- versus Miss-trials: POS was significantly higher than expected by chance in 77 virtual sensors in source-space (all FDR-corrected $p < .046$; Figure 2b). Separate analyses, in which the trials were stratified for pre-stimulus alpha power, confirmed that the POS results were not confounded by power (16/889 FDR-corrected significant virtual sensors; smallest $p < .001$; see Supplementary Materials and Figure S4). Brain source results revealed significant phase effects in the left occipital cortex (second

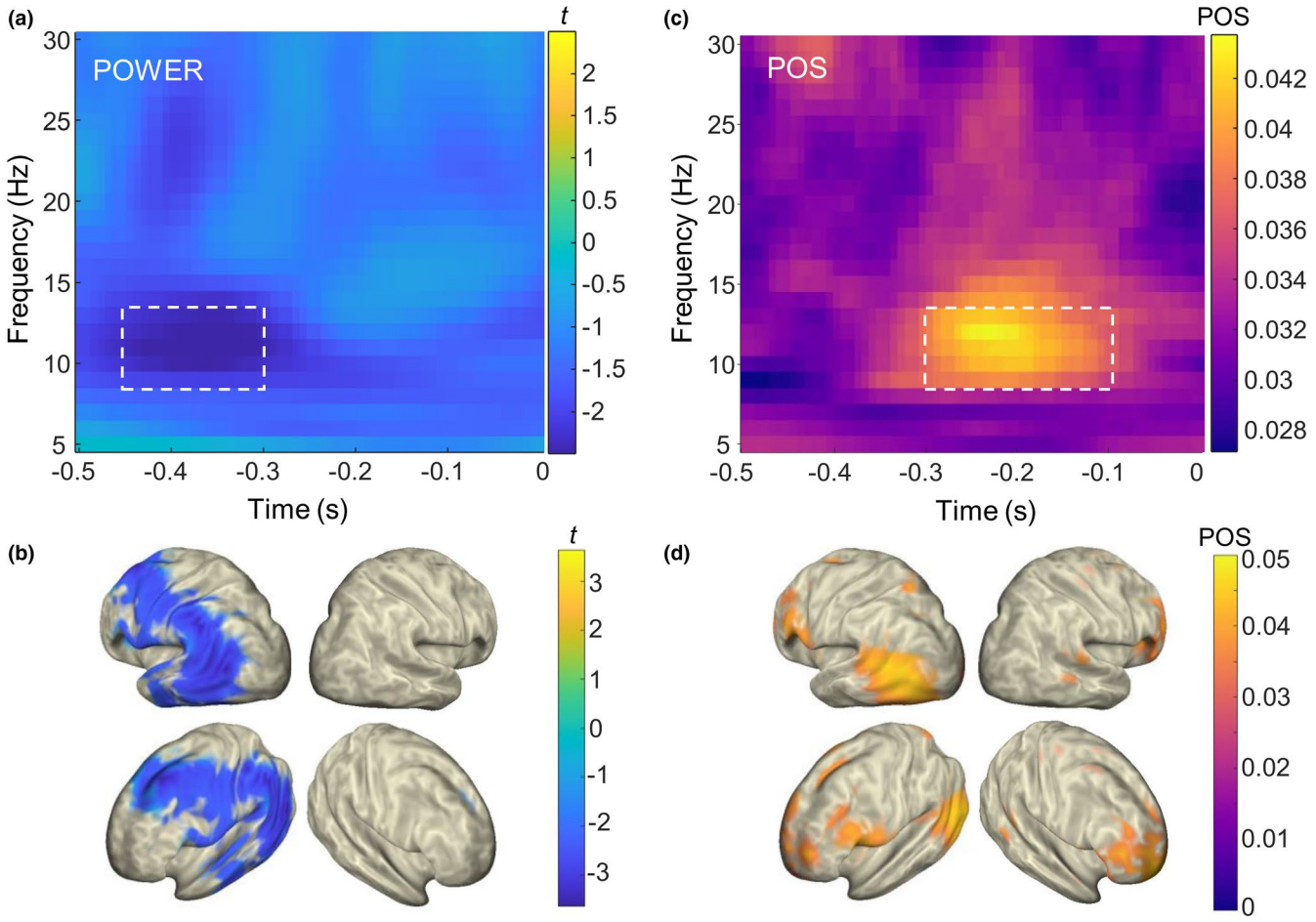

FIGURE 2 Hits versus Misses in pre-stimulus alpha oscillations. (a) Time-frequency plot of t values comparing power between Hits and Misses in the pre-stimulus window (time 0 = stimulus onset), averaged over significant virtual sensors in the cluster, at the time-frequency range highlighted by the white rectangle (i.e., from −0.45 to −0.3 s, from 9 to 13 Hz). b) Source plot of significant t values with a threshold at $p = .01$ averaged over the alpha band (9–13 Hz) and the pre-stimulus time window from −0.45 and −0.3 s. The white rectangle indicates the time-frequency range of interest represented in source plots. (c) Time-frequency plot of POS values, averaged over significant virtual sensors (FDR corrected; Benjamini & Hochberg, 1995). The white rectangle indicates the time-frequency range of interest considered in the statistical analysis and represented in d). (d) Source plots of significant POS values averaged over the alpha frequency band (9–13 Hz) and a pre-stimulus time window from −0.3 to −0.1 s. In (b) and (d), for visualization purposes, data has been interpolated over virtual sensors

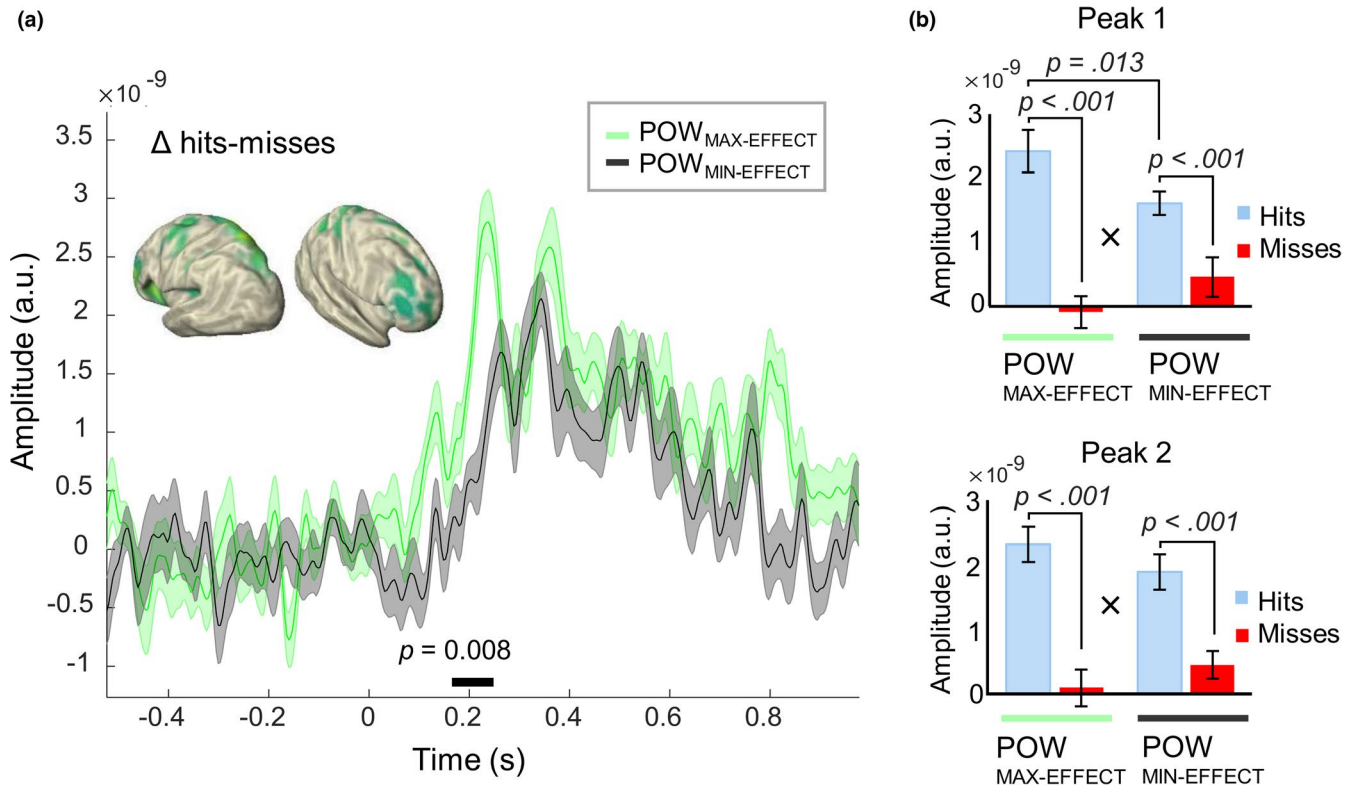

FIGURE 3 Effect of pre-stimulus alpha power on stimulus-evoked response. (a) Time course of ERFs for Hits-Misses difference (baseline corrected for visualization purpose), significantly larger for $POW_{MAX\text{-}EFFECT}$ than $POW_{MIN\text{-}EFFECT}$ from ~0.17 to 0.25 s, averaged over significant virtual sensors represented in source plot (inset). Within-subject *SE* in shaded error bars (Morey, 2008). (b) Results of 2 × 2 rm-ANOVA with factors Response (Hits, Misses) and Power ($POW_{MAX\text{-}EFFECT}$, $POW_{MIN\text{-}EFFECT}$), on ERF Peak 1 (top) and Peak 2 (bottom), indicating a main effect of Response (Hits > Misses) and a Response × Power interaction (Peak 1: Hits in $POW_{MAX\text{-}EFFECT}$ > $POW_{MIN\text{-}EFFECT}$). Significant post-hoc comparisons are indicated by *p* values (Bonferroni corrected). Within-subject *SE* in error bars (Morey, 2008)

highest POS value in BA 19; $POS_{MAX(2)} = 0.046$; MNI coordinates in mm: −50, −80, 10) but also in prefrontal cortex in the right hemisphere (maximum POS value located in right BA 10; $POS_{MAX(1)} = 0.047$; MNI coordinates in mm: 25, 55, −20). In sum, both pre-stimulus power and phase affected perceptual outcome, but we found different neural generators for the observed effects. Both pre-stimulus power and phase effects involved occipital-temporal regions contralateral to the stimulus location, but the phase effects also extended to prefrontal cortex ipsilateral to stimulation.

In a next step, we investigated the influence of the observed pre-stimulus effects on the subsequent post-stimulus evoked responses. If pre-stimulus alpha-band power and phase are functionally relevant for conscious perception, then we would expect them to impact not only the behavioural outcome, but also the neurophysiological correlate of conscious access, namely the post-stimulus evoked response. To this end, we selected subsets of trials in which the pre-stimulus alpha-band power- and phase impact was maximized and minimized, respectively (30% trials each for $POW_{MAX\text{-}EFFECT}$, $POW_{MIN\text{-}EFFECT}$, $POS_{MAX\text{-}EFFECT}$ and $POS_{MIN\text{-}EFFECT}$, see Methods and Figures S6–S9 for single-subject data on sorted trial for $POS_{MAX\text{-}EFFECT}$ and $POS_{MIN\text{-}EFFECT}$). First, the trial sorting for the maximal and minimal phase effects was done based on two separate regions of interest in the left occipital cortex and in the right prefrontal cortex (for single-subject data see Figures S6–S9). As a confirmation of our trial-sorting approach, we found strong pre-stimulus effects in the max-effect trial subsets (cluster-corrected $p = .002$ in $POW_{MAX\text{-}EFFECT}$; in $POS_{MAX\text{-}EFFECT}$, 595/889 FDR-corrected significant virtual sensors for trial-sorting by left occipital—smallest $p < .001$—and 589/889 for trial-sorting by right prefrontal—smallest $p < .001$; Figure S5). By contrast, there were (almost) no significant effects in the min-effect trial subsets (no cluster identified in $POW_{MIN\text{-}EFFECT}$; for $POS_{MIN\text{-}EFFECT}$, 0/889 FDR-corrected significant virtual sensors for trial-sorting by left occipital—smallest $p = .91$—and 5/889 for trial-sorting by right prefrontal—smallest $p = .036$). For all trial subsets, we found significant post-stimulus differences in the ERFs between Hits and Misses (all cluster-corrected $p = .002$). Importantly, however, the post-stimulus ERF difference (ΔHits − Misses) was significantly greater for the $POW_{MAX\text{-}EFFECT}$ versus $POW_{MIN\text{-}EFFECT}$ trial subset (cluster-corrected $p = .008$). This effect on ERFs occurred between 0.17 s and 0.25 s after stimulus onset.

It engaged different brain regions—parietal and frontal areas of both hemispheres (Figure 3a)—than those of the pre-stimulus power effect *per se*, which mostly involved left occipital-parietal areas (Figure 2b). Consistent with the cluster-based analysis, the repeated-measures ANOVAs on the two ERF peaks (at peak 1 = 240 ± 20 ms and at peak 2 = 360 ± 20 ms) showed significant interactions between Response (Hits vs. Misses) and Effect ($POW_{MAX\text{-}EFFECT}$ vs. $POW_{MIN\text{-}EFFECT}$; Peak 1: $F_{1,19} = 17.8$, $p < .001$, $\eta_p^2 = 0.48$; Peak 2: $F_{1,19} = 4.5$, $p = .047$, $\eta_p^2 = 0.19$; Figure 3b). Bonferroni-corrected post-hoc comparisons showed that the response for Hits in $POW_{MAX\text{-}EFFECT}$ was larger than in $POW_{MIN\text{-}EFFECT}$ only for the first peak (Peak 1: $p = .013$; Peak 2: $p = .7$). Furthermore, for both peaks we observed a main effect of Response (Peak 1: $F_{1,19} = 19.9$, $p < .001$, $\eta^2 = 0.51$; Peak 2: $F_{1,19} = 24$, $p < .001$, $\eta^2 = 0.56$) showing a significantly larger response for Hits than Misses in both power levels, while the factor Effect alone was not significant (Peak 1: $F_{1,19} = 0.5$, $p = .47$, $\eta^2 = 0.02$; Peak 2: $F_{1,19} = 0.04$, $p = .84$, $\eta^2 < 0.1$). Similarly, in the second analysis, in which trial sorting was based on the average over all significant virtual sensors, instead of the single one showing the strongest effect, a greater ERF-difference (ΔHits − Misses) in $POW_{MAX\text{-}EFFECT}$ versus $POW_{MIN\text{-}EFFECT}$ was observed, between 0.41 s and 0.52 s after stimulus onset (cluster-corrected $p = .042$).

By contrast, the pre-stimulus phase effects had less influence on the post-stimulus evoked response. There were no significant differences between the $POS_{MAX\text{-}EFFECT}$ versus $POS_{MIN\text{-}EFFECT}$ trial subsets for the post-stimulus ERF-difference (ΔHits − Misses), neither when tested with a cluster-based analysis across all virtual sensors and time points (trial sorting by left occipital: smallest cluster-corrected $p = .875$; trial sorting by right prefrontal: smallest cluster-corrected $p = 1$) nor when tested at the peaks on the virtual sensors where we found the effects for the pre-stimulus power trial subsets (all $p > .05$ for the interaction between Response and Effect; Figure S10). In line with these results, no effect on ERFs was found when trial sorting was performed by averaging over all significant virtual sensors (cluster-corrected $p > .85$; Figure S11a), nor when trial sorting was performed by averaging over the whole time-frequency range of interest (cluster-corrected $p > .18$; Figure S11b). In sum, we only found a post-stimulus influence on the ERFs for the pre-stimulus power effects but not for the pre-stimulus phase effects.

4 | DISCUSSION

In the present work, we successfully replicated previous findings of pre-stimulus alpha-band activity effects on perceptual outcome in a near-threshold visual detection task. Hits differed from Misses in both features of pre-stimulus alpha-band oscillations, power and phase, as well as in the visual-evoked response. Importantly, we observed distinct brain sources linked to pre-stimulus alpha activity. Whereas pre-stimulus alpha-band power effects occurred in sensory-related brain regions contralateral to the presentation of the stimulus, the effect of pre-stimulus alpha-band phase also involved higher order regions in prefrontal cortex ipsilateral to stimulation. Furthermore, pre-stimulus alpha power (but not phase) had an impact on the stimulus-evoked response, boosting the neural response of successful conscious perception.

4.1 | Pre-stimulus alpha power involves lateralized occipital-temporal areas

As expected, we observed stronger pre-stimulus alpha-band power preceding Miss-trials compared to Hits. Our result is consistent with the hypothesis of an inhibitory effect of alpha-band activity on conscious perception (Jensen & Mazaheri, 2010; Klimesch et al., 2007), which has been further confirmed by several recent findings (Benwell, Keitel, et al., 2018; Benwell, Tagliabue, et al., 2017; Iemi & Busch, 2018; Iemi et al., 2017; Limbach & Corballis, 2016; Samaha et al., 2017). The difference in pre-stimulus alpha-band power between Hits and Misses was strongest around 0.4 s before stimulus onset and occurred in the left occipital-temporal cortex. This finding is in line with reports of sensory-related, "occipital alpha," suggested by topographical EEG maps that indicate the involvement of posterior electrodes (Hanslmayr et al., 2007; Romei et al., 2008; Thut et al., 2006), as well as by previous MEG studies, which identified occipital and parietal areas involved in the alpha-band power modulation for visual discrimination ability (van Dijk et al., 2008) or visual-temporal integration (Wutz et al., 2014). Furthermore, it is worth noting that the target stimulus in the detection task was always presented in the right side of the screen; therefore, the lateralization of the effect contralateral to target presentation, together with the involvement of posterior brain areas, strongly support the hypothesis of a key role of alpha-band power in modulating local excitability of sensory-related brain regions (Jensen & Mazaheri, 2010).

4.2 | Prestimulus alpha phase involves both occipital and prefrontal areas

On top of the alpha-band power modulations, we also observed significant effects of pre-stimulus alpha-band phase on visual perception: Hit- and Miss-trials were linked to opposite phases just before stimulus onset. This result successfully replicates previous findings (Busch et al., 2009; Mathewson et al., 2009) and corroborates the interpretation

of pulsed inhibition exerted by alpha-band oscillations (Jensen & Mazaheri, 2010; Mathewson et al., 2011). In terms of brain sources, our POS results revealed the involvement of left occipital areas but also of right frontal regions. Intriguingly, our finding on pre-stimulus alpha phase match the results of a previous EEG study (Dugué et al., 2011), in which pre-stimulus alpha-band activity in both posterior and frontal-central electrodes predicted phosphene perception evoked by near-threshold transcranial magnetic stimulation. The relevance of a "frontal alpha" for visual attention and perception, in addition to the more classical "occipital alpha", has been proposed previously, although it was mostly based on EEG topographies (Busch et al., 2009; Zoefel & VanRullen, 2017). Our findings support this hypothesis by providing evidence at the brain source level.

4.3 | Pre-stimulus alpha power—but not phase—boosts post-stimulus visual-evoked response

The repeated presentation of identical near-threshold stimuli gave rise to different neural responses, which strongly depended on conscious report: Whereas the evoked response in the ERFs was almost absent on Miss-trials, we observed a clear evoked response for Hits, peaking at 0.24 s and 0.36 s after stimulus onset. These latencies are consistent with event-related potential components reported by (Busch et al., 2009), which employed a similar near-threshold visual detection task, and more generally with the timing of the neural response commonly associated to perceptual awareness (Fisch et al., 2009; Sergent et al., 2005). The opposite pattern for the Hits versus Misses contrast observed in ERF amplitude (i.e., Hits > Misses) and in post-stimulus alpha power (i.e., Misses > Hits) suggest that the two phenomena are subtended by different mechanisms. At the brain source level, the contrast between Hits and Misses revealed a first peak mainly located in occipital areas of the left hemisphere. The lateralization of this early response is consistent with the lateralized presentation of the stimuli, which were always on the right side of the screen, suggesting that the first peak may reflect aspects related to sensory processing. At the latency of the second peak, neural activity extensively spread also into temporal and parietal areas of the right hemisphere, with a peak in the supramarginal gyrus in parietal cortex. Taken together, both temporal and spatial features of our results on the stimulus-evoked response are in line with the well-established neural signature of conscious perception after stimulus onset, which involves several stages along the visual pathway, from early sensory areas to higher-order prefrontal cortex (Dehaene & Changeux, 2011; Lamme, 2006; Sanchez et al., 2020; Van Vugt et al., 2018).

Considering that the effects of both features of pre-stimulus alpha oscillations (i.e., power and phase) significantly shaped perceptual outcome, we expect them to impact also the post-stimulus evoked response. Importantly, we report evidence that the visual-evoked response is boosted by pre-stimulus alpha-band power. When the effect of pre-stimulus alpha-band power is strong, that is, when selecting Hit-trials with low pre-stimulus alpha power and Miss-trials with high pre-stimulus alpha power, we observed a greater difference between Hits and Misses in the ERFs than when the same effect was minimized. The similar results obtained when sorting trials by averaging over all significant virtual sensors, instead of the single one showing the strongest effect, indicates that the effect of pre-stimulus alpha power on the evoked response was robust, and not dependent on the trial sorting procedure. The latency of the effects suggests that pre-stimulus alpha power mainly contributes to the first peak of the ERFs, that is, around 0.24 s after stimulus onset, and involves higher-order neural activations in parietal and frontal areas. This result is in line with a large body of evidence indicating a link between pre-stimulus oscillations and post-stimulus evoked potentials (Mazaheri & Jensen, 2008), starting with pioneering work in the early 90s (Başar et al., 1998). Specifically, a relationship between pre-stimulus EEG alpha power and event-related potential has been described both at early (e.g., N1 component, Roberts et al., 2014; P1 component, Fellinger et al., 2011) as well as at later latencies (e.g., P3 component, Ergenoglu et al., 2004; Min & Herrmann, 2007), not only in the visual but also in the somatosensory domain (Zhang & Ding, 2010). Importantly, our approach which aims to maximize and minimize the effect of alpha power on the hits/misses contrast underscores the functional relevance of source-level pre-stimulus alpha power for perceptual awareness, extending previous reports limited to detecting its effect on trial outcome (Benwell, Keitel, et al., 2018; Benwell, Tagliabue, et al., 2017; Busch et al., 2009; Iemi & Busch, 2018; Iemi et al., 2017; Limbach & Corballis, 2016; Samaha et al., 2017).

The same analysis conducted on the effects of pre-stimulus alpha phase on ERFs led to no significant post-stimulus modulations. We detected no difference between ERFs computed when the phase opposition was maximal or minimal. One hypothesis is that alpha phase effects on the evoked response have been underestimated due to the reduction of a great amount of data to specific spatial-spectral-temporal points of interest. Nevertheless, we accounted for this possible concern by running additional analyses with different trial sorting methods that considered the entire time-frequency range of interest as well as the whole cluster of significant virtual sensors; the negative results further support that there is no significant effect of pre-stimulus alpha phase on the stimulus-evoked response. This indicates that, although pre-stimulus alpha-band

phase can account for variability in perceptual outcome, it does not seem to affect the stimulus-evoked response. This result suggests a distinct role of pre-stimulus alpha phase as compared to alpha power, yet, it challenges its functional relevance for conscious perception. Indeed, the role of pre-stimulus alpha-band phase has been recently questioned by several studies leaving an open issue on whether such inconsistency may be due to variability in methodological approaches, experimental factors or physiological reasons (Benwell, Keitel, et al., 2018; Benwell, Tagliabue, et al., 2017; Ruzzoli et al., 2019). Here, however, we did observe a significant effect of pre-stimulus alpha-band phase on perceptual outcome: the employment of a detection paradigm similar to the one by Busch et al. (2009), which led to significant alpha-band phase effects also in subsequent studies (Busch & Van Rullen, 2010; Chaumon & Busch, 2014), may suggest that at least a portion of the variability in the literature in detecting pre-stimulus phase effects could be due to experimental factors, such as the eccentricity of the target stimulus in the visual field (as already pointed out by Ruzzoli et al. (2019) or stimulus duration (Benwell, Tagliabue, et al., 2017).

5 | CONCLUSIONS

We provide evidence of non-overlapping, distinct brain sources accounting for the effects of pre-stimulus alpha-band power and phase on perceptual outcome. Moreover alpha-band power and phase had distinct impact on the stimulus-evoked response. Taken together, our findings suggest that the two features of alpha oscillations—power and phase—may reflect distinct mechanisms of perceptual modulation in the visual domain, highlighting the functional relevance of pre-stimulus alpha power for conscious access while questioning the functional role of alpha phase.

ACKNOWLEDGEMENTS

This research was supported by the European Research Council to P.R. and N.W. (ERC StG 283404 – WIN2CON), by a Lise-Meitner grant from the Austrian Science Fund (FWF) awarded to A.W. (grant agreement number: M2496) and by the Italian Ministry of Health to A.Z. (Ricerca Corrente). The authors thank Sheri Dawoon Choi for help with data collection.

CONFLICT OF INTEREST

The authors declare no competing interest.

AUTHOR CONTRIBUTIONS

P.R. conceived the study and performed the experiment. N.W. conceived the study and wrote the article. A.W. and A.Z. performed data analysis and wrote the article.

PEER REVIEW

The peer review history for this article is available at https://publons.com/publon/10.1111/ejn.15138.

DATA AVAILABILITY STATEMENT

Preprocessed data and analysis code are openly available at https://osf.io/269y5/.

ORCID

Agnese Zazio https://orcid.org/0000-0002-1395-9005

REFERENCES

Ai, L., & Ro, T. (2014). The phase of prestimulus alpha oscillations affects tactile perception. *Journal of Neurophysiology*, *111*, 1300–1307.

Andersen, L. M., Pedersen, M. N., Sandberg, K., & Overgaard, M. (2016). Occipital MEG activity in the early time range (<300 ms) predicts graded changes in perceptual consciousness. *Cerebral Cortex*, *26*, 2677–2688.

Bąsar, E., Rahn, E., Demiralp, T., & Schürmann, M. (1998). Spontaneous EEG theta activity controls frontal visual evoked potential amplitudes. *Electroencephalography and Clinical Neurophysiology*, *108*, 101–109.

Baumgarten, T. J., Schnitzler, A., & Lange, J. (2016). Prestimulus alpha power influences tactile temporal perceptual discrimination and confidence in decisions. *Cerebral Cortex*, *26*, 891–903. https://doi.org/10.1093/cercor/bhu247

Benjamini, Y., & Hochberg, Y. (1995). Controlling the false discovery rate: A practical and powerful approach to multiple testing. *Journal of the Royal Statistical Society Series B (Statistical Methodology)*, *57*, 289–300.

Benwell, C. S. Y., Keitel, C., Harvey, M., Gross, J., & Thut, G. (2018). Trial-by-trial co-variation of pre-stimulus EEG alpha power and visuospatial bias reflects a mixture of stochastic and deterministic effects. *European Journal of Neuroscience*, *48*, 2566–2584.

Benwell, C. S. Y., Tagliabue, C. F., Veniero, D., Cecere, R., Savazzi, S., & Thut, G. (2017). Pre-stimulus EEG power predicts conscious awareness but not objective visual performance. *eNeuro*, *4*, e0182–e217.

Berens, P. (2009). CircStat: A MATLAB toolbox for circular statistics. *Journal of Statistical Software*, *31*,1–21.

Brainard, D. H. (1997). The psychophysics toolbox. *Spatial Vision*, *10*, 433–436.

Busch, N. A., Dubois, J., & Vanrullen, R. (2009). The phase of ongoing EEG oscillations predicts visual perception. *Journal of Neuroscience*, *29*, 7869–7876.

Busch, N. A., & Van Rullen, R. (2010). Spontaneous EEG oscillations reveal periodic sampling of visual attention. *Proceedings of the National Academy of Sciences of the United States of America*, *107*, 16048–16053.

Chaumon, M., & Busch, N. A. (2014). Prestimulus neural oscillations inhibit visual perception via modulation of response gain. *Journal of Cognitive Neuroscience*, *26*, 2514–2529.

Dehaene, S., & Changeux, J. P. (2011). Experimental and theoretical approaches to conscious processing. *Neuron*, *70*, 200–227. https://doi.org/10.1016/j.neuron.2011.03.018

Dugué, L., Marque, P., & VanRullen, R. (2011). The phase of ongoing oscillations mediates the causal relation between brain excitation and visual perception. *Journal of Neuroscience*, *31*, 11889–11893.

Ergenoglu, T., Demiralp, T., Bayraktaroglu, Z., Ergen, M., Beydagi, H., & Uresin, Y. (2004). Alpha rhythm of the EEG modulates visual detection performance in humans. *Cognitive Brain Research*, *20*, 376–383.

Fellinger, R., Klimesch, W., Gruber, W., Freunberger, R., & Doppelmayr, M. (2011). Pre-stimulus alpha phase-alignment predicts P1-amplitude. *Brain Research Bulletin*, *85*, 417–423.

Fisch, L., Privman, E., Ramot, M., Harel, M., Nir, Y., Kipervasser, S., Andelman, F., Neufeld, M. Y., Kramer, U., Fried, I., & Malach, R. (2009). Neural "Ignition": Enhanced activation linked to perceptual awareness in human ventral stream visual cortex. *Neuron*, *64*, 562–574. https://doi.org/10.1016/j.neuron.2009.11.001

Frey, J. N., Mainy, N., Lachaux, J., Mu, N., Bertrand, O., & Weisz, N. (2014). Selective modulation of auditory cortical alpha activity in an audiovisual spatial attention task. *Journal of Neuroscience*, *34*, 6634–6639. https://doi.org/10.1523/JNEUROSCI.4813-13.2014

Hanslmayr, S., Aslan, A., Staudigl, T., Klimesch, W., Herrmann, C. S., & Bäuml, K. H. (2007). Prestimulus oscillations predict visual perception performance between and within subjects. *NeuroImage*, *37*, 1465–1473. https://doi.org/10.1016/j.neuroimage.2007.07.011

Hanslmayr, S., Gross, J., Klimesch, W., & Shapiro, K. L. (2011). The role of alpha oscillations in temporal attention. *Brain Research Reviews*, *67*, 331–343.

Henry, M. J., & Obleser, J. (2012). Frequency modulation entrains slow neural oscillations and optimizes human listening behavior. *Proceedings of the National Academy of Sciences of the United States of America*, *109*, 20095–22100.

Iemi, L., & Busch, N. A. (2018). Moment-to-moment fluctuations in neuronal excitability bias subjective perception rather than strategic decision-making. *eNeuro*, *5*(3), ENEURO.0430-17.2018. https://doi.org/10.1523/ENEURO.0430-17.2018

Iemi, L., Chaumon, M., Crouzet, S. M., & Busch, N. A. (2017). Spontaneous neural oscillations bias perception by modulating baseline excitability. *Journal of Neuroscience*, *37*, 807–819.

Jensen, O., Gips, B., Bergmann, T. O., & Bonnefond, M. (2014). Temporal coding organized by coupled alpha and gamma oscillations prioritize visual processing. *Trends in Neurosciences*, *37*, 357–369.

Jensen, O., & Mazaheri, A. (2010). Shaping functional architecture by oscillatory alpha activity: Gating by inhibition. *Frontiers in Human Neuroscience*, *4*, 1–8.

Klimesch, W., Sauseng, P., & Hanslmayr, S. (2007). EEG alpha oscillations: The inhibition-timing hypothesis. *Brain Research Reviews*, *53*, 63–88.

Lachaux, J. P., Rodriguez, E., Martinerie, J., & Varela, F. J. (1999). Measuring phase synchrony in brain signals. *Human Brain Mapping*, *8*, 194–208.

Lamme, V. A. F. (2006). Towards a true neural stance on consciousness. *Trends in Cognitive Sciences*, *10*(11), 494–501. https://doi.org/10.1016/j.tics.2006.09.001

Limbach, K., & Corballis, P. M. (2016). Prestimulus alpha power influences response criterion in a detection task. *Psychophysiology*, *53*, 1154–1164. https://doi.org/10.1111/psyp.12666

Linkenkaer-Hansen, K., Nikulin, V. V., Palva, S., Ilmoniemi, R. J., & Palva, J. M. (2004). Prestimulus oscillations enhance psychophysical performance in humans. *Journal of Neuroscience*, *24*, 10186–10190.

Maris, E., & Oostenveld, R. (2007). Nonparametric statistical testing of EEG- and MEG-data. *Journal of Neuroscience Methods*, *164*, 177–190.

Mathewson, K. E., Gratton, G., Fabiani, M., Beck, D. M., & Ro, T. (2009). To see or not to see: prestimulus α phase predicts visual awareness. *Journal of Neuroscience*, *29*, 2725–2732.

Mathewson, K. E., Lleras, A., Beck, D. M., Fabiani, M., Ro, T., & Gratton, G. (2011). Pulsed out of awareness: EEG alpha oscillations represent a pulsed-inhibition of ongoing cortical processing. *Frontiers in Psychology*, *2*, 1–15. https://doi.org/10.3389/fpsyg.2011.00099

Mazaheri, A., & Jensen, O. (2008). Asymmetric amplitude modulations of brain oscillations generate slow evoked responses. *Journal of Neuroscience*, *28*, 7781–7787.

Min, B., & Herrmann, C. S. (2007). Prestimulus EEG alpha activity reflects prestimulus top-down processing. *Neuroscience Letters*, *422*, 131–135.

Morey, R. D. (2008). Confidence intervals from normalized data: A correction to Cousineau (2005). *Tutorials in Quantitative Methods for Psychology*, *4*, 61–64.

Nolte, G. (2003). The magnetic lead field theorem in the quasi-static approximation and its use for magnetoencephalography forward calculation in realistic volum conductors. *Physics in Medicine & Biology*, *48*, 3637–3652.

Oostenveld, R., Fries, P., Maris, E., & Schoffelen, J. M. (2011). FieldTrip: Open source software for advanced analysis of MEG, EEG, and invasive electrophysiological data. *Computational Intelligence and Neuroscience*, *2011*, 1–9. https://doi.org/10.1155/2011/156869

Pelli, D.G. (1997). The VideoToolbox software for visual psychophysics: transforming numbers into movies. *Spat*, *10*, 437–442.

Rassi, E., Wutz, A., Müller-Voggel, N., & Weisz, N. (2019). Prestimulus feedback connectivity biases the content of visual experiences. *Proceedings of the National Academy of Sciences of the United States of America*, *116*, 16056–16061.

Roberts, D. M., Fedota, J. R., Buzzell, G. A., Prasuraman, R., & McDonald, C. G. (2014). Prestimulus oscillations in the alpha band of the EEG are modulated by the difficulty of feature discrimination and predict activation of a sensory discrimination process. *Journal of Cognitive Neuroscience*, *26*, 1615–1628. https://doi.org/10.1162/jocn_a_00569

Romei, V., Brodbeck, V., Michel, C., Amedi, A., Pascual-Leone, A., & Thut, G. (2008). Spontaneous fluctuations in posterior alpha-band EEG activity reflect variability in excitability of human visual areas. *Cerebral Cortex*, *18*, 2010–2018.

Ruhnau, P., Hauswald, A., & Weisz, N. (2014). Investigating ongoing brain oscillations and their influence on conscious perception – Network states and the window to consciousness. *Frontiers in Psychology*, *5*, 1–9.

Ruzzoli, M., Torralba, M., Fernandeza, L. M., & Soto-Faraco, S. (2019). The relevance of alpha phase in human perception. *Cortex*, *120*, 249–268. https://doi.org/10.1016/j.cortex.2019.05.012

Samaha, J., Iemi, L., & Postle, B. R. (2017). Prestimulus alpha-band power biases visual discrimination confidence, but not accuracy. *Consciousness and Cognition*, *54*, 47–55.

Sanchez, G., Hartmann, T., Fuscà, M., Demarchi, G., & Weisz, N. (2020). Decoding across sensory modalities reveals common supramodal signatures of conscious perception. *Proceedings of the National Academy of Sciences of the United States of America*, *117*, 7437–7446.

Schalk, G. (2015). A general framework for dynamic cortical function: The function-through-biased-oscillations (FBO) hypothesis. *Frontiers in Human Neuroscience*, *9*, 1–10.

Sergent, C., Baillet, S., & Dehaene, S. (2005). Timing of the brain events underlying access to consciousness during the attentional blink. *Nature Neuroscience*, *8*, 1391–1400.

Thut, G., Nietzel, A., Brandt, S. A., & Pascual-Leone, A. (2006). α-band electroencephalographic activity over occipital cortex indexes visuospatial attention bias and predicts visual target detection. *Journal of Neuroscience*, *26*, 9494–9502.

van Dijk, H., Schoffelen, J.-M., Oostenveld, R., & Jensen, O. (2008). Prestimulus oscillatory activity in the alpha band predicts visual discrimination ability. *Journal of Neuroscience*, *28*, 1816–1823.

Van Veen, B. D., van Drongelen, W., Yuchtman, M., & Suzuki, A. (1997). Localization of brain electrical activity via linearly constrained minimum variance spatial filtering. *IEEE Transactions on Biomedical Engineering*, *44*, 867–880.

Van Vugt, B., Dagnino, B., Vartak, D., Safaai, H., Panzeri, S., Dehaene, S., & Roelfsema, P. R. (2018). The threshold for conscious report: Signal loss and response bias in visual and frontal cortex. *Science*, *360*, 537–542. https://doi.org/10.1126/science.aar7186

VanRullen, R. (2016a). Perceptual cycles. *Trends in Cognitive Sciences*, *20*, 723–735. https://doi.org/10.1016/j.tics.2016.07.006

VanRullen, R. (2016b). How to evaluate phase differences between trial groups in ongoing electrophysiological signals. *Frontiers in Neuroscience*, *10*, 1–22. https://doi.org/10.3389/fnins.2016.00426

Weisz, N., Wühle, A., Monittola, G., Demarchi, G., Frey, J., Popov, T., & Braun, C. (2014). Prestimulus oscillatory power and connectivity patterns predispose conscious somatosensory perception. *Proceedings of the National Academy of Sciences of the United States of America*, *111*, 417–425.

Wutz, A., Melcher, D., & Samaha, J. (2018). Frequency modulation of neural oscillations according to visual task demands. *Proceedings of the National Academy of Sciences of the United States of America*, *115*(6), 1346–1351. https://doi.org/10.1073/pnas.1713318115

Wutz, A., Weisz, N., Braun, C., & Melcher, D. (2014). Temporal windows in visual processing: "prestimulus brain state" and "poststimulus phase reset" segregate visual transients on different temporal scales. *Journal of Neuroscience*, *34*, 1554–1565. https://doi.org/10.1523/JNEUROSCI.3187-13.2014

Wyart, V., & Tallon-Baudry, C. (2008). Neural dissociation between visual awareness and spatial attention. *Journal of Neuroscience*, *28*, 2667–2679.

Zazio, A., Schreiber, M., Miniussi, C., & Bortoletto, M. (2020). Modelling the effects of ongoing alpha activity on visual perception: The oscillation-based probability of response. *Neuroscience and Biobehavioral Reviews*, *112*, 242–253. https://doi.org/10.1016/j.neubiorev.2020.01.037.

Zhang, Y., & Ding, M. (2010). Detection of a weak somatosensory stimulus: Role of the prestimulus mu rhythm and its top-down modulation. *Journal of Cognitive Neuroscience*, *22*, 307–322. https://doi.org/10.1162/jocn.2009.21247

Zoefel, B., & VanRullen, R. (2017). Oscillatory mechanisms of stimulus processing and selection in the visual and auditory systems: State-of-the-art, speculations and suggestions. *Frontiers in Neuroscience*, *11*, 1–13. https://doi.org/10.3389/fnins.2017.00296

SUPPORTING INFORMATION

Additional supporting information may be found online in the Supporting Information section.

How to cite this article: Zazio A, Ruhnau P, Weisz N, Wutz A. Pre-stimulus alpha-band power and phase fluctuations originate from different neural sources and exert distinct impact on stimulus-evoked responses. *Eur J Neurosci*. 2021;00:1–13. https://doi.org/10.1111/ejn.15138